EUROPEAN ORGANIZATION FOR NUCLEAR RESEARCH

CERN - LABORATORY II

Lab II/BT/Int./73-5

DESIGN STUDY OF THE SPS BEAM DUMPING SYSTEM

by

P.E. Faugeras, C.G. Harrison and G.H. Schröder

Geneva - 26th July, 1973

CONTENTS

1. Introduction

An internal beam dumping system is needed for the SPS, in order to prevent uncontrolled loss of the beam in the accelerator. Several possible dumping schemes have been studied and compared in Ref. (1), and the method using fast kicker magnets has been chosen. The beam dumping system will use a pair of kicker magnets, which deflect the beam vertically onto the absorber blocks, and the beam will be dumped in one SPS revolution.

It has been shown in [1] that dumping a low emittance beam of 10^{13} ppp at 400 GeV/c leads to severe thermal problems in the absorber blocks. In particular, dumping the beam with fast kickers induces in the absorber blocks instantaneous temperature rises. These depend on the proton density distributions in the beam and the material used for the block and can be at least as high as 1000^{o}C in case of aluminium. Although the values of these temperature spikes cannot be calculated with good accuracy, they are certainly higher than permitted for a reliable absorber block design. It is not possible to blow up the beam before the dumping process starts in order to reduce these spikes,as this is not compatible with a fast emergency beam dumping system. It is therefore necessary to spread the beam over the front surface of the absorber block during the 23 μs long dumping process. This report describes the method which will be used and which proceeds in two steps :

1. Instead of giving a constant kick to the beam, as described in Ref. (1), the pulse forming networks (pfn's) which excite the vertically deflecting kickers will be designed such that they give a current pulse which exhibits oscillations on its flat top. The amplitude of these oscillations can be of the order of ±10% of the mean flat top current. The deflected beam will no longer be dumped on a small area of the front face of the absorber block equal to the beam cross section, but will oscillate vertically during the dumping process. The fast kicker magnets (MKDV) and their pfn's will be described in Chapter 2.

2. In addition, the beam will be swept horizontally during dumping, by means of additional magnets which are excited by a linearly rising current pulse. These magnets are called "sweepers" or MKDH. The pulse will be generated by a capacitor discharge, starting at the same time as the pulse exciting the kickers MKDV, and reaching its maximum after more than 24 μs. Chapter 3 deals with these additional sweeper magnets, and shows that for suitable values of their parameters, a horizontal sweep of about 25 mm at 400 GeVc can be achieved.

Both methods must be used at the same time if one wants to reduce the temperature spikes in the absorber block *) to a safe level. Together they ensure that the beam, during dumping, is spread over an area of the front face of the absorber block TIDV, which is of the order of 10 times the beam cross-section at 400 GeV/c when the latter corresponds to the design emittance (5). The temperature spikes will be reduced accordingly.

2. The Vertically Deflecting Kickers (MKDV)

2.1 Main Parameters

The MKDV consist of two full aperture ferrite magnets each about 2.5 m long. The excitation current for each magnet is generated by the discharge of a pulse forming network (pfn) through the magnet into a matched terminating resistor. The pfn and magnet are connected by a matched transmission line which is about 150 m long and is made of five coaxial cables of 15Ω in parallel. The characteristic impedance of the system has been defined in Ref. (1, Chapter 3) and is

$$Z = 3.0\ \Omega\ .$$

A schematic layout of the magnets is shown in Fig. 1 and the main parameters are listed in Table 1. Due to a small shift in their position in the SPS lattice the aperture of the magnets is slightly increased

*) The absorber blocks 1 and 2 of Ref. (1) are now designated as TIDH and TIDV according to the Lab II abbreviation code - (drawing 8002-010-11).

as compared to the values given in Ref. [1].

2.2 Response of the magnet

The equivalent circuit of the magnet must be optimized in order to obtain

- a short risetime of the kick strength
- good pulse transmission properties
- a low reflection coefficient.

The kick risetime determines the dumping efficiency, which is defined as the ratio of the number of protons dumped on the absorber block to the total number of protons in the beam (Ref. 1, Chapter 3.3). The shorter the risetime of the kick strength, the higher is the dumping efficiency. For instance a kick risetime of 1 μs leads to an efficiency of about 99%. Good pulse transmission properties and a low reflection coefficient are also required, because reflections strongly distort the oscillations, which are deliberately superimposed on the mean flat top of the current pulse.

The magnet response has been investigated for different types of magnet circuits, using the computer program described in Ref. (2). The magnet pulse response has been studied first when discharging a pfn of 26 equal cells via a transmission line of 150 m length through the magnet into a matched resistor. Such a pfn delivers a rectangular current pulse without oscillations (see Chapter 2.4) which facilitates the analysis of the magnet response. Losses in the cable of 0.8 dB/100 m at 10 MHz were taken into account. The overall inductance of the magnet was taken to be 2.4 μH (see Chapter 2.3).

The results are similar to those described in [2] and can be summarized as follows :

- the purely inductive magnet is unsuitable for our requirements, because it gives a relatively long risetime of 1.4 μs (0% to 100%), and large voltage reflections of maximum amplitude 76 %.

- an inductive magnet with a front cell before and a matching capacity behind it is also unsuitable, because the risetime is still 1.4 μs (0% to 100%). The voltage reflections (18% maximum) are nevertheless acceptable;

- a reduction of reflections and a shorter kick risetime are obtained simultaneously if the magnet is equivalent to a lumped delay line with the same characteristic impedance as the pfn (see Fig.2). For such a magnet the kick risetime is determined by the risetime of the pulse given by the pfn and by the travelling time of the pulse through the magnet. The amplitude of the reflections decreases when increasing the number of cells, but above a certain number, the improvement per added cell becomes marginal. The number of cells is moreover limited by cost considerations.

For our purpose a five-section magnet with a front matching cell has a pulse response which is adequate. The pulse shape of the kick strength is shown in Fig. 3. The kick risetime is 0.97 μs (0% - 100%), and the voltage reflections have a maximum amplitude of 17%.

2.3 Magnet configuration

The total magnet inductance and hence the kick risetime is influenced by the magnet configuration. A C-shaped magnet has a higher inductance than a window frame configuration. Since the field is strongly non-uniform near the outer conductor of a C-shaped magnet, the gap width has to be increased. However, for our application a field non-uniformity of about 1% is acceptable, which gives an increase in gap width of only 10 %. On the other hand the C-configuration has important advantages :

- outer conductor at ground potential
- better high voltage insulation to earth
- lower impedance with the SPS beam: a rough estimate gives 1.4 Ω, as compared to 83 Ω for the window frame shape.

Therefore, the C-configuration was chosen.

In view of the relatively high flux density of 0.14 T in the magnet gap, a nickel zinc ferrite with especially high saturation induction will be used (Philips, Type FXC 8C1C, induction for 10 Oe and at 23° C > 0.3 T). In addition, this material has a low coercive force (Hc < 0.25 Oe). The one turn deflection due to the remanent field in the magnet will be smaller than 0.016 mrad for 10 GeV/c protons at injection and the corresponding amplitude of the coherent vertical betatron oscillation will be smaller than 0.85 mm for the nominal value of $Q_V = 27.55$.

The ferrite thickness will be 60 mm, to keep the flux density in the core low. Calculations with the computer program MAGNET [3] have shown, that by adding a 5 × 1 mm shim at the pole profile near the outer conductor and by increasing the gap width from 51 mm to 56 mm, one can obtain a field non-uniformity smaller than 1% over a width of 51 mm (see Fig. 4). These calculations are, however, approximate, as the program MAGNET deals only with static magnetic fields, and neglects the end effects.

2.4 The pulse generator

The rectangular current pulse normally used for the excitation of kicker magnets is often generated in a LC-ladder network (pfn), consisting of cells of equal capacitance and inductance. Oscillations on the flat top of the current pulse can be generated by increasing the time constant

$$\tau_n = \sqrt{L_n C_n}$$

of each cell of the pfn with respect to the preceding one, starting with the cell adjacent to the discharge switch. All cells must have the same characteristic impedance

$$Z_c = \sqrt{\frac{L_n}{C_n}} \quad .$$

A high number of cells generates a high number of oscillations of small amplitude, whereas with a small number of cells one gets a small number of oscillations of large amplitude. Because of the increasing time constants of the cells, the frequency of the oscillation decreases

during the pulse. The amplitude distribution of the oscillations can be influenced by the function, with which the time constants increase.

The pfn was then designed using the following criteria :

- the amplitude of the oscillations shall be up to 10% of the mean flat top current;
- all cells shall be assembled from as small as possible a number of different capacitor units;
- the assembly of the capacitors must be easy, e.g. no series connection of the capacitors;
- it must be possible to rearrange the capacitors in the existing tank such as to produce a pulse without oscillations.

A number of pfn's with different distributions of the time constants and different number of cells have been studied by means of the same computer program [2]. The best results were obtained with a pfn of 14 cells and time constants increase according to the series

$$\tau,\ 2\tau,\ 3\tau,\ \ldots\ldots\ldots\ 14\tau\ .$$

The equivalent circuit of the pfn is given in Fig. 5 and the kick response of the 5-section magnet is shown in Fig. 6. The transmission line is again assumed to be 150 m long and to have an attenuation of 0.8 dB/100 m at 10 MHz.

The oscillation has maximum amplitudes of +7% and -10%, and the kick rise-time up to the minimum required deflection is 0.9 μs.

The amplitudes of the oscillations near the beginning of the kick pulse are reduced due to the low pass filter behaviour of the magnet. This can be avoided with a smaller number of cells, but then the amplitude of

the oscillations becomes too large.

The capacitors of the pfn can be rearranged in their tank such that a pfn with 26 equal cells is formed. The response of this latter pfn together with the 5-section magnet with a front cell is given in Fig. 3.

One important problem of the pulse generator consists in finding a switch, which can hold a voltage of up to 60 kV and carry a 23 μs long current pulse of up to 10 kA. We favour a composite switch, called "thyragnitron" which is made of a deuterium thyratron of normal design by-passed by three ignitrons in series. The thyratron provides only the required steep current rise and the precise turn on, whereafter the ignitrons progressively take over the discharge current. A "thyragnitron", using an EEV CX 1171 thyratron [6] paralleled by 3 National Tube NL 1039 A ignitrons, has been tested for more than 10^6 pulses at 4 kA flat top current and 23 μs pulse length without any sign of deterioration [4].

Nevertheless, it remains to be confirmed experimentally that a "thyragnitron" using a CX 1191 thyratron *) can produce current pulses of up to 10 kA amplitude and is not affected by the proposed oscillations superimposed on the flat top of the current pulse.

To test this, a prototype pfn will be constructed, together with a short version of the kicker magnet.

To get the same displacement on the absorber block for all momenta of the circulating beam, the charging voltage of the pfn must be varied proportionally to the beam momentum. This would require a variation of the charging voltage of a factor of 40, whereas the thyratron is only capable of a voltage variation of a factor of 10. At a voltage below about 6 kV, the thyratron CX 1191 can no longer be triggered reliably. Therefore, at an injection momentum of 10 GeV/c the deflection will be about four times the nominal deflection. When raising the proton momentum the voltage will be kept constant up to 40 GeV/c, giving a deflection, which is inversely proportional to the

---

*) and three EEV 7703 ignitrons [6]

momentum and which reaches the nominal value at 40 GeV/c (see Fig. 7). Above 40 GeV/c the voltage tracks the momentum and the deflection remains constant.

3. The horizontally deflecting kickers (MKDH)

3.1 Rate of rise of excitation current

The sweeper magnets MKDH are excited by a capacitor discharge which generates a half sine wave current pulse. If it were desired that the part of the sine wave which is used to sweep the beam during the dumping process were practically linear, the frequency of the discharge would have to be about 3.6 kHz (Fig. 8, curve 1). But then the spatial distribution of the protons on the front surface of the absorber block would not be homogeneous. It would be given by Fig. 6 with the time in abscissa changed in horizontal deflection. This inhomogeneity is due to the decreasing frequency of the oscillations on the flat top of the kick given by MKDV. This can be compensated by using more than the linear part of the sine wave during the dumping time. The decrease of frequency for the vertical oscillation is more or less compensated by a decrease in dI/dt towards the end of the horizontal sweep.

The best results are obtained if the excitation frequency is 9 kHz (see Fig. 9). For 25 mm horizontal deflection in front of the absorber block TIDV, one can then calculate that the beam is spread over an area, which is of the order of 10 times the beam cross-section at 400 GeV/c and for the design emittances[5]. The temperature spikes will be reduced accordingly.

The choice of a frequency of 9 kHz has the further advantage that for a given deflection the maximum current is reduced by about a factor 2, as compared to 3.6 kHz. Also the capacitor bank is much smaller at 9 kHz, but the required voltage of the system is slightly higher.

3.2 Position of the MKDH in the lattice

The MKDH can be placed either upstream or downstream of the MKDV. The apertures of the magnets placed downstream have always to be increased to allow for the deflection generated by the magnets placed upstream. An increase in aperture corresponds for both the MKDV and MKDH to an increase in excitation current and hence in higher demands on the capabilities of the switches. The MKDV switches are probably nearer to the limit of their capabilities than the MKDH switches, which will be ignitrons and can handle currents of up to 100 kA[6]. Therefore, the MKDH is placed immediately downstream of the MKDV. A schematic layout is given in Fig.1.

3.3 Main Parameters

Table 2 gives the parameters of the MKDH magnets for a momentum of 400 GeV/c and a horizontal displacement of 25 mm at the front face of the absorber block TIDV. The MKDH apertures are calculated according to the assumptions of Ref. 1, para. 2.2. In addition, as explained in chapter 2.4, a beam which is deflected by four times the nominal vertical deflection angle must pass through the MKDH.

Three different construction principles are compared in Table 2:

i) a ferrite magnet mounted in a vacuum tank (column 1)
ii) a laminated iron magnet with a ceramic vacuum chamber in the gap (column 2)
iii) a laminated iron magnet mounted in a vacuum tank (column 3).

A metallic vacuum chamber in the magnet gap cannot be used because of the strong field perturbations due to the eddy currents : a corrugated INCONEL vacuum chamber of 0.4 mm wall thickness and with corrugations of 5 mm width and 3 mm height reduces the dipolar component of the field by 50% and induces a sextupolar component of up to 20% [13].

The ferrite magnet (column 1) allows only moderate fields of, at most, 0.2T in the gap because of the low saturation induction in the ferrite and is therefore comparatively long. However, due to the high elec-

trical resistivity of ferrite, a higher working voltage than for iron magnets is permitted. In our application such a magnet need not be sub-divided into modules, each with its own pulse generator.

For the iron laminated magnets (columns 2 and 3), we limit the maximum current to 30 kA and the maximum voltage against earth to about 3kV (1, para. 4.1). The total length of the magnet is then chosen according to the current limit, and the number of modules according to the voltage limit. It is also assumed that the laminations are sufficiently thin to neglect the eddy current effects.

For column 2, the ceramic vacuum chamber in the magnet gap is assumed to have a rectangular cross-section and a wall thickness of 5 mm. A clearance of 1 mm between chamber and yoke is also taken into account.

As compared to the iron laminated magnets, the ferrite magnet has the following drawbacks:

- the cost is 25 % higher
- the remanent kick strength is higher
- the required space in LSS4 is longer.

The choice between the two versions of iron magnets (column 2 and 3) is somewhat difficult. Although a ceramic vacuum chamber of rectangular cross-section seems to be feasible according to previous experience, [14] making it would require development work. On the other hand, a laminated magnet working under vacuum might have a high outgassing rate due to the thin laminations and the epoxy insulated coil. However, due to its smaller gap, the excitation energy of such a magnet is 30 % lower than the one of a magnet with a ceramic vacuum chamber. This reduces considerably the requirements on the switch and is therefore an important advantage.

Tests are underway to determine the outgassing rate of a stack of laminations, and the first results are encouraging. We therefore assume for the rest of

this note that the MKDH will be built as iron laminated magnets working under vacuum.

3.4 Frequency dependent effects

Under a.c. excitation the mean induction B_m in an iron lamination of thickness 2a is lower than the surface magnetization B_s, and is given by[7,8] :

$$B_m = B_s \left(\frac{\sqrt{2}}{x} \sqrt{\frac{\cosh x - \cos x}{\cosh x + \cos x}} \right) \simeq B_s \left(\frac{\sqrt{2}}{x} \right) \text{for large } x$$

where $x = 2a/\delta$, and δ is the skin depth :

$$\delta = \sqrt{\frac{2}{\mu_r \mu_o \omega \sigma}}$$

where μ_r is the relative permeability, ω the angular frequency of the excitation and σ the conductivity of the iron. For the required MKDH gap field $B_o = 0.66$ T, the mean yoke magnetization will be of the same magnitude, if the yoke width is the same as the gap width, and so, to avoid surface saturation of the laminations, the lamination thickness 2a must be chosen such that

$$B_s < B_{\text{saturation}} \simeq 2\text{T}, \quad \text{i.e.} \quad \frac{B_s}{B_m} < 3.$$

This criterion gives a lamination thickness of the order of 0.3 mm.

This eddy current effect leads to a lower effective permeability, μ_{eff}, for a.c. excitation

$$\mu_{eff} = \mu_r \frac{B_m}{B_s}$$

where μ_r is the relative permeability at the surface induction B_s. Consequently, the ampere-turns in the iron core are higher than in the case of d.c. excitation. Computer calculations using program MAGNET [3] and

introducing the effective permeability μ_{eff} show that under a.c. excitation about 0.8% of the ampere-turns can be expected in the iron, as compared with 0.1% for d.c. excitation. This leads to a corresponding decrease in the magnet inductance. Such changes in the excitation current and inductance are acceptable for our application. The eddy current heating in the laminations is proportional to the conductivity of the iron, which should thus be low.

3.5 Magnet construction

As with the MKDV's a field in the gap uniform to within only $\pm$ 1% can be tolerated and hence the MKDH's will also have a C-shape configuration.

Since the outer conductor of a C-shape magnet is non-inductive, it can be bolted rigidly to the yoke. The coil will be centre fed and the magnet split into two halves, as is often done in septum magnets [9]: this minimizes the necessary insulation thickness on the inner conductor. This thickness was assumed to be 2 mm (Fig. 10a). The field distribution in the gap, calculated with program MAGNET[3] does not depend very strongly on the current distribution in the conductors (Fig. 10b). As two MKDH's are required, the overall field distribution seen by the SPS beam can be improved by putting the first magnet with the opening of its C-yoke facing the SPS centre and the second magnet facing outwards from the centre (Fig. 11).

The remanent field was estimated for a coercive force of 0.5 Oe and has a maximum value of $4.3 \cdot 10^{-4}$ T on the magnets centre line. For 10 GeV/c protons, at injection the one turn deflection is smaller than 0.031 mrad and the corresponding amplitude of the coherent horizontal betatron oscillation will be smaller than 1.10 mm for the nominal value of $Q_H = 27.60$.

With a current pulse of 30 kA amplitude at an excitation frequency of 9 kHz and a repetition period of 4 sec, the rms magnet current is 88A. The skin effect raises the conductor resistance to 1.6 mΩ and so the average conductor dissipation is 14 W, generated uniformly along the length of the conductor. The eddy current loss in the yoke under the

the same conditions is 6 W. The eddy current loss in the non-magnetic end plates is difficult to estimate, but should be of the same magnitude. If good thermal contact between the outer conductor and the yoke and between the yoke and the vacuum tank can be achieved, this dissipation can be conducted away with temperature differences of less than 10°C, making cooling unnecessary.

A force with a peak value of $2 \cdot 10^4$ N/m acts on the conductors during the pulse. As the pulse is very short, the momentum produced is only 0.55 N.s/m, but the long term effects of this force, in particular possible damage to the insulation, are unknown, and will be studied experimentally on a model.

3.6 The pulse generator

The required half-sine wave pulse will be produced by the discharge of a capacitor bank through the cable and magnet inductances, followed by a clamping process to limit the voltage reversal on the capacitors (Figs. 12 and 13). Ideally, the cable inductance should be negligible, but in practice the two inductances will be comparable. This implies a capacitance of about 66 μF and a charging voltage of about 8 kV. As the magnet is centre-fed the whole supply circuit must be balanced with respect to ground and the capacitor terminals must both be insulated from the case. The stray inductance of the capacitors must be low to minimize ringing effects.

The HV switch must stand off 8 kV and conduct 30 kA with an initial rate of rise of current of 1.7 kA/μs. Because of the high dI/dt, the use of thyristors is economically unattractive[10] and so the large ignitron BK178[6] will be used. This has already been employed in similar installations[9,11].

To prevent recharging of the capacitors after the first quarter of the sine-wave and to provide a rapid decay of the magnet current, a diode clamp or crowbar is employed. The initial rate of rise of the diode

current is also large, possibly 5-10 kA/μs (Fig. 13), though it will be limited by stray inductance in the diode and the crowbar resistor. The crowbar resistance is 50 mΩ and gives a peak inverse voltage of 1.5 kV. The total circuit resistance for the crowbar operation will be about 100 mΩ, giving a time constant for the decay of 50 μs. The average dissipation in the crowbar resistor will be 250 W with 1 pulse every 4 s.

3.7 The transmission line

To connect the balanced power supply to the magnet terminals, two balanced, low inductance conductors are required plus an earth shield. Cables with suitable voltage ratings are found to have inductances in the range 70-200 nH/m, so that over a 150 m run, even 6 cables in parallel have an inductance comparable to that of the magnet. It is undesirable to raise the number of cables above 6, because of the costs involved. Three types of cable were considered: striplines, cross-connected four-conductor cables (balanced quad) and shielded coaxial cables (triaxial).

Striplines have the advantage of very low inductance but they are not commercially available at the required voltage rating.

Four conductor power cable is readily available at voltages up to 11 kV (a.c.). When cross-connected, however, its inductance is rather high, typically 150-200 nH/m and this would necessitate too many cables in parallel.

A cable consisting of four thin coaxial cables surrounded by an earth shield has been proposed [12]. This ingenious approach gives a net inductance of only 33 nH/m and is particularly attractive since, in principle, two cables should be sufficient. Such cables used for a balanced supply suffer from an unbalanced capacitance between the outer conductor and the ground shield, which may lead to spurious resonances. This can be avoided with an even number of cables by connecting half of them with reversed polarity.

Although the net cable resistance is small, ca. 50 mΩ, the damping effect is not entirely negligible and the charging voltage must be increased by about 10% above the nominal value to achieve the 30 kA peak current.

4. Conclusion

It has been shown that in order to deal with the low emittance, high intensity beam at momenta of up to 400 GeV/c foreseen for the SPS, the beam dumping system must be made of two types of magnet :

1) a pair of fast kickers, the MKDV's,deflecting the beam vertically. These kickers will be excited by a special, fast rising current pulse, 23 μs long, with the deliberately superimposed oscillations on its flat top.

2) Two additional magnets, the MKDH's,excited by half a sine wave, will sweep the beam horizontally during the dumping process.

Therefore, the dumped beam will be spread over an area of the front face of the absorber block which will be of the order of 10 times the beam cross-section for the design emittance at 400 GeV. The temperature spikes induced in the absorber block during dumping will then be reduced to a safe level.

Nevertheless, several points need to be checked from the hardware point of view and require prototype work. In particular, for the MKDV, one has to verify the reliability of the "thyragnitron" switch, for pulses of up to 10 kA, and the feasibility of oscillations on the pulse flat top. A short magnet model is also necessary in order to measure the pulse propagation properties and the field distribution in the gap. This model will be installed later on in LSS5 and used as a kicker for measuring the QV of the machine. A full length prototype of the MKDH will also be built, to test the magnet construction principles and assess the voltage holding capability, the vacuum behaviour, the cooling efficiency and the field uniformity. If this prototype proves to be satisfactory, it could be used as a spare unit of the final MKDH.

All this prototype work is under way.

Acknowledgements

We would like to express our appreciation to B. de Raad and W.C. Middelkoop for their constant support and guidance. This work has also benefited from discussions with other members of the BT Group, especially with P. Sievers.

References

1) P.E. Faugeras, W.C. Middelkoop, B. de Raad, G. Schröder and P. Sievers, Beam Dumping in the SPS, CERN Lab II/BT/Int./72-5.

2) P.E. Faugeras, Calculations on the SPS Inflector Magnet and its Pulse Generator, CERN Lab II/BT/72-1.

3) C. Iselin, MAGNET, Programme for Two-dimensional Magnetic Fields including Saturation, CERN Computer Program Library T600.

4) P.E. Faugeras, H. Kuhn, J.-P. Zanasco, Generation of High Current, Long Duration Rectangular Pulses, to be published.

5) The 300 GeV Programme, CERN 1050, 14.1.72.

6) English Electric Valve Co., Product Data Handbook 1971.

7) D. Reistad, Simple Expressions to Evaluate Eddy Current Effects in Laminated Magnets, CERN ISR/BT/68-42.

8) K. Küpfmüller, Theoretische Elektrotechnik, 8e Auflage, Springer-Verlag, Berlin, 1965.

9) H. van Breugel, R. Cuénot, S. Hérin and B. Kuiper, The Septum Magnets for the Fast Ejection System of the Serpukhov 70 GeV Proton Synchrotron, CERN PS/FES/72-4.

10) P.S. Harley, Westinghouse Brake and Signal Co. Ltd., private communication.

11) G. Gruber, R. Grüb and B. Langeseth, The High Voltage Capacitor Discharge System and the 200 kJ, 500 kA Pulsed Current Supply for the Magnetic Horn and Reflectors of the CERN Neutrino Beam, CERN NPA/Int./69-13.

12) Felten and Guilleaume, Kabelwerk AG, Köln.

13) F. Schäff, Analytic Approximations to Eddy Current Field Components in quasi-rectangular Bending Magnet Vacuum Chambers, SI/MAE-Note/71-4.

14) H. Kuhn, private communication.

Table 1 : Main parameters of the vertically deflecting kickers MKDV

beam displacement in front of absorber block (TIDV)	(mm)	44
deflection angle	(mrad)	0.52
kickstrength at 400 GeV/c	(Tm)	0.69
gap width w (vertical)	(mm)	56
gap height h (horizontal)	(mm)	75
number of modules		2
module length	(m)	2.56
magnetic field	(T)	0.135
inductance per module	(μH)	2.4
characteristic impedance	(Ω)	3.0
maximum peak current	(kA)	10.0
maximum pfn charging voltage	(kV)	60

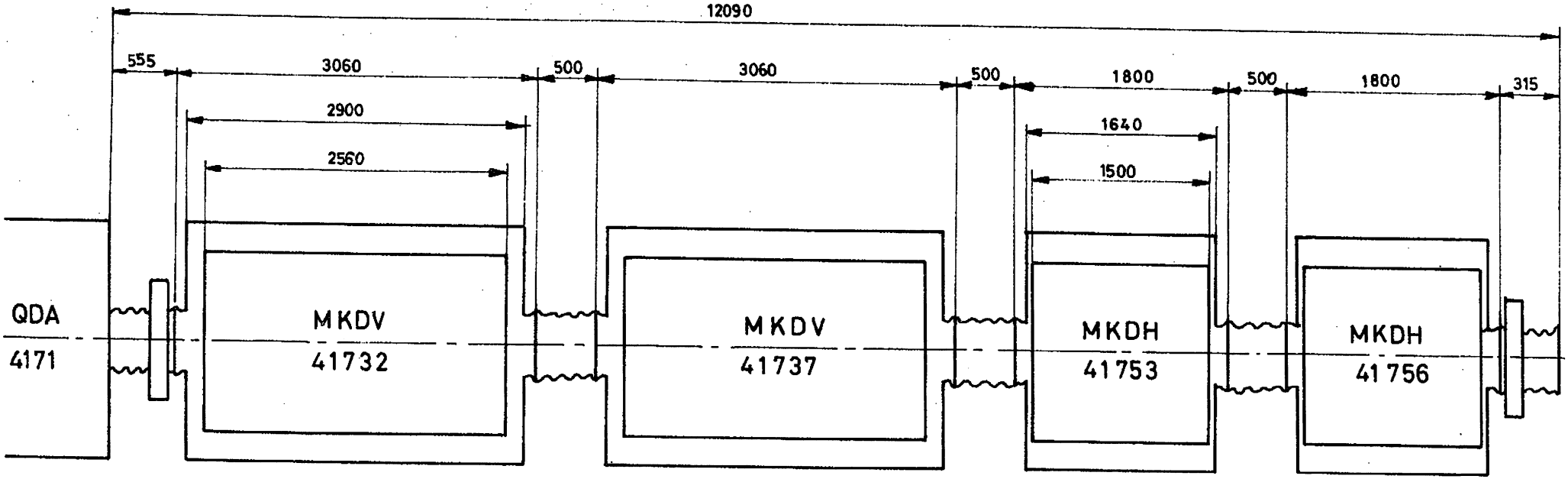

Fig.1

LSS 4 Beam dumping system layout

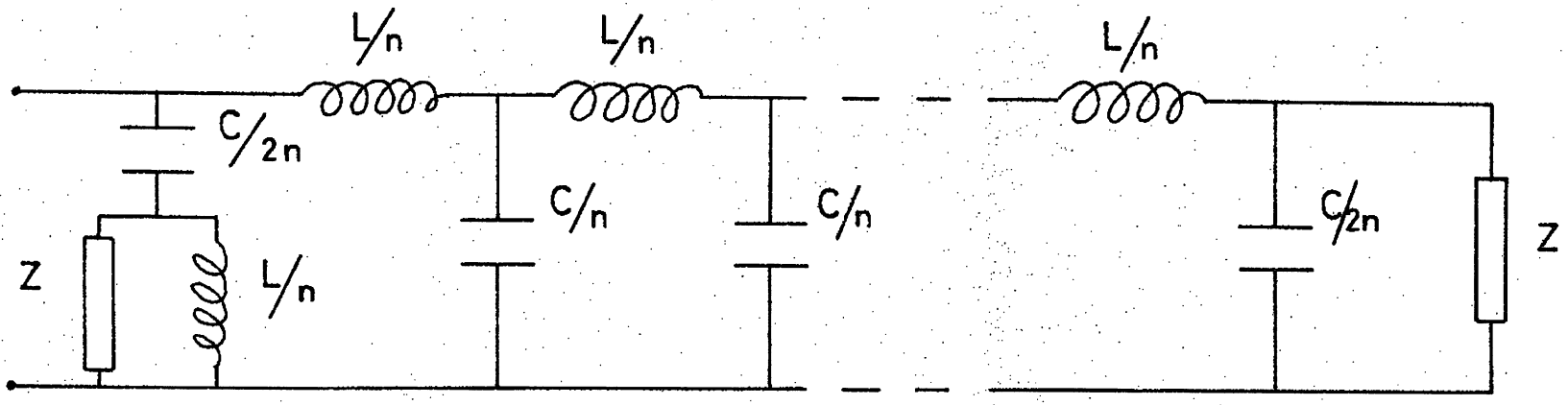

Lumped delay line magnet (C - shape) with front cell

n = number of sections	= 5
L = total magnet inductance	= 2·4 μH
Z = characteristic impedance	= 3 Ω
C = L/Z^2	= 0·267 μF

Fig 2

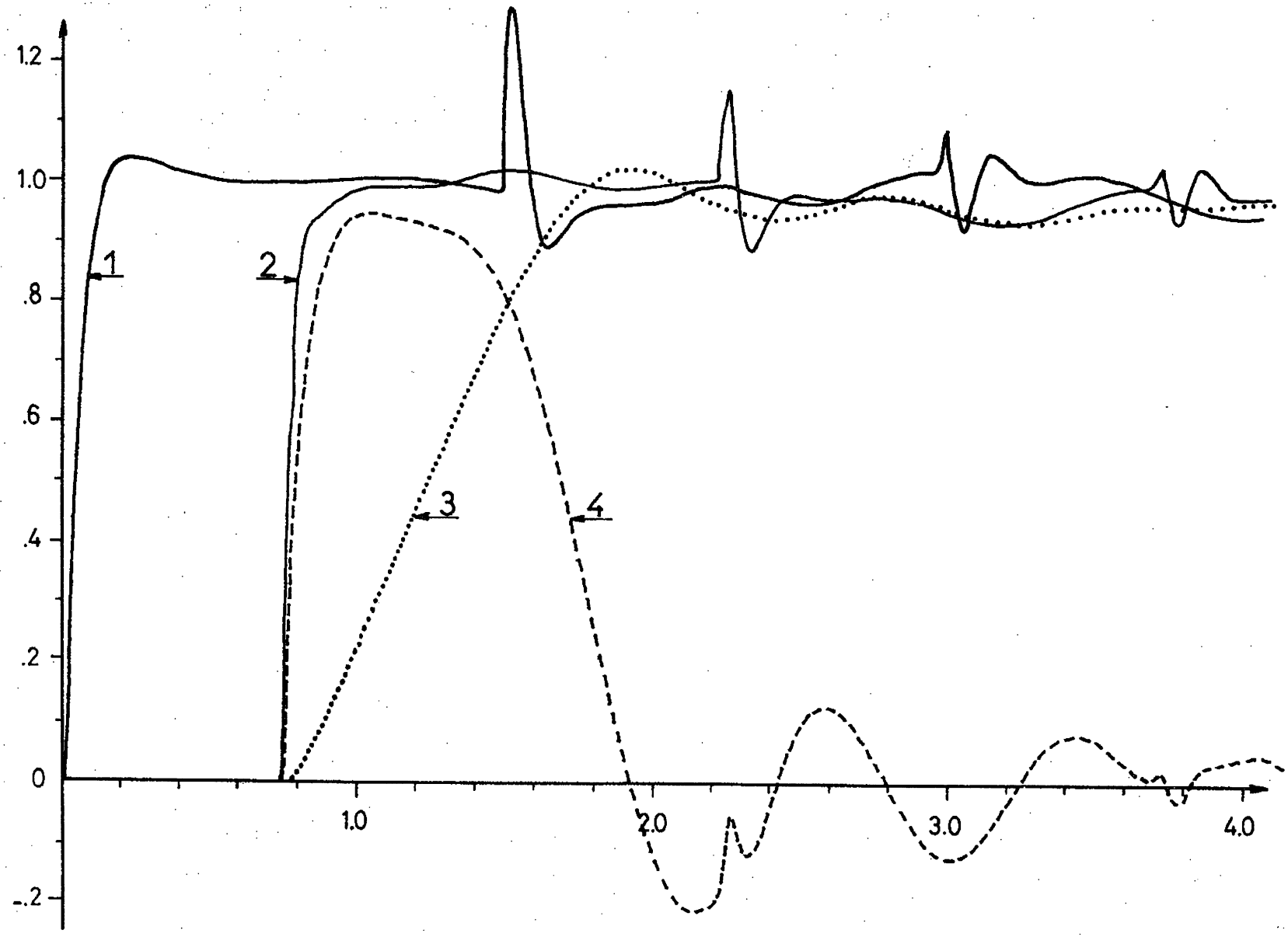

1) Voltage pulse at pfn output.
2) Voltage pulse at magne input.
3) Kick strength.
4) Time derivative of kick strength. ≡ voltage across magnet.

(all values are normalized

Fig.3 KICK RESPONSE OF THE 5 SECTION MAGNET.

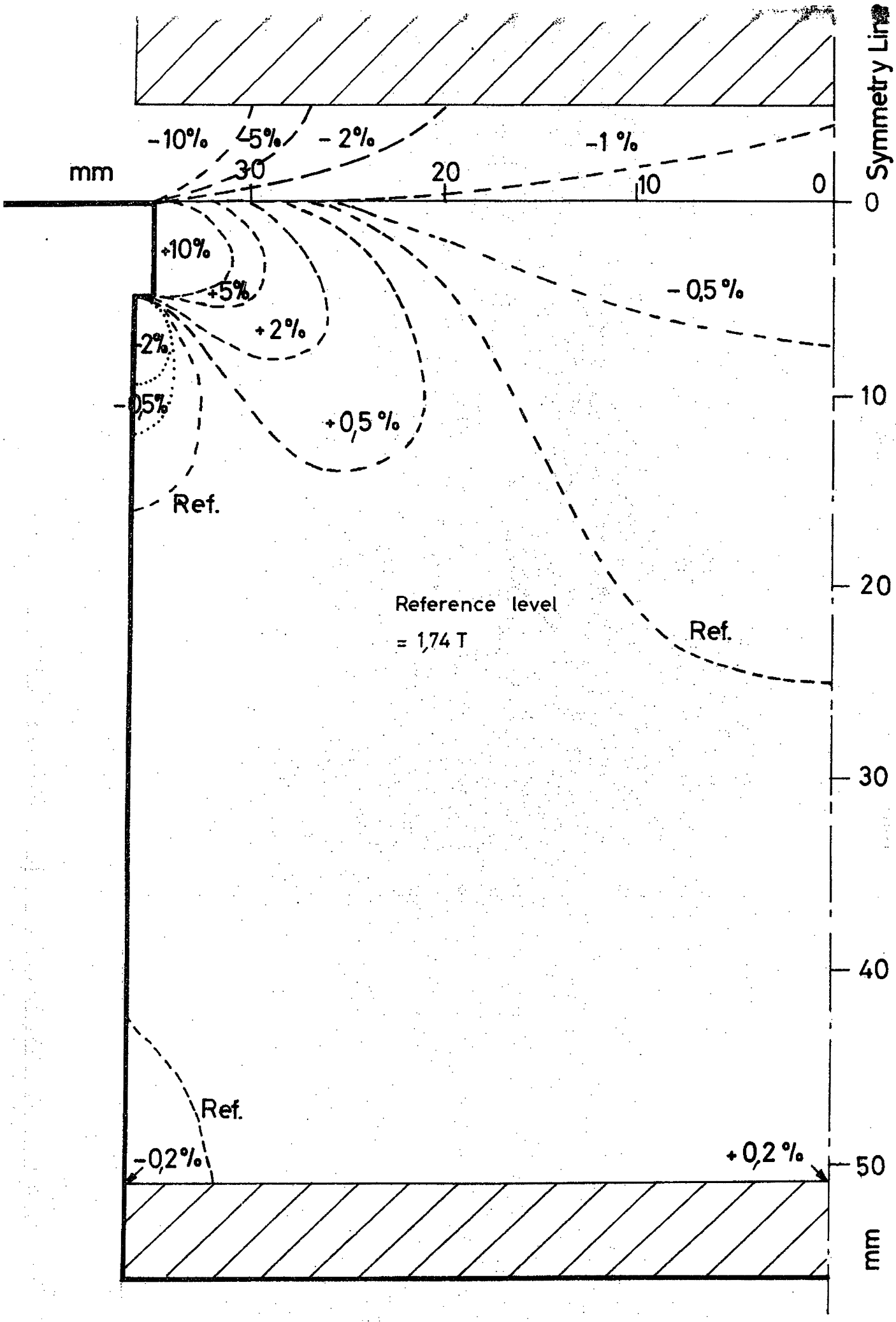

Fig 4 Non uniformity of the field inside the magnet gap (MKDV)

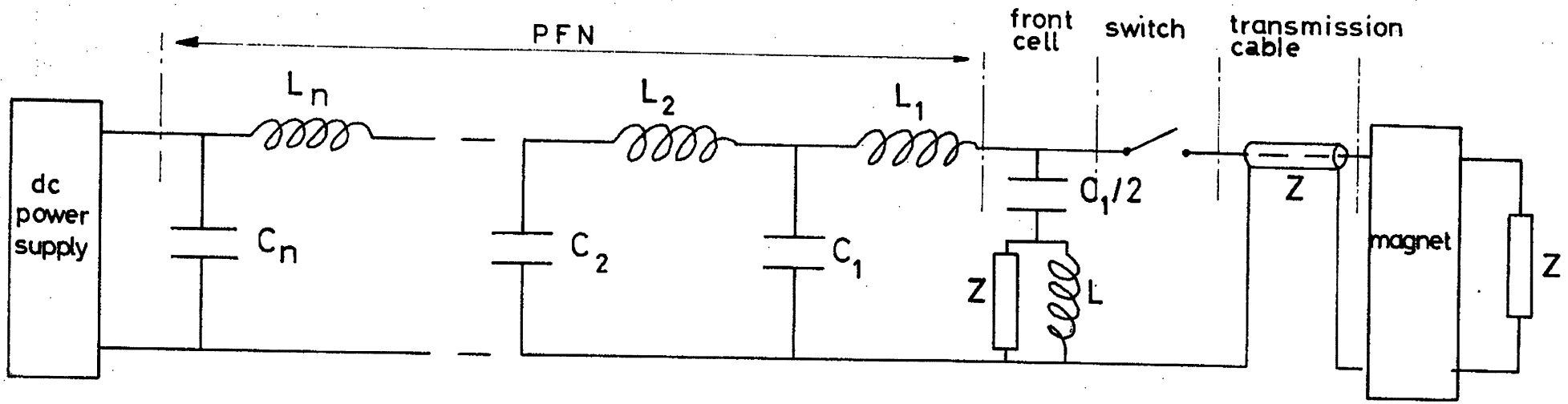

Pulse generator circuit

$C_1 = 40\,\mu F$ $\quad L_1 = 0.36\,\mu H$

$C_2 = 2 * C_1$ $\quad L_2 = 2 * L_1$

$C_3 = 3 * C_1$ $\quad L_3 = 3 * L_1$

$C_n = n * C_1$ $\quad L_n = n * L_1$

$n = 14$ $\quad Z = \sqrt{\frac{L}{C}} = 3\,\Omega$

Fig. 5

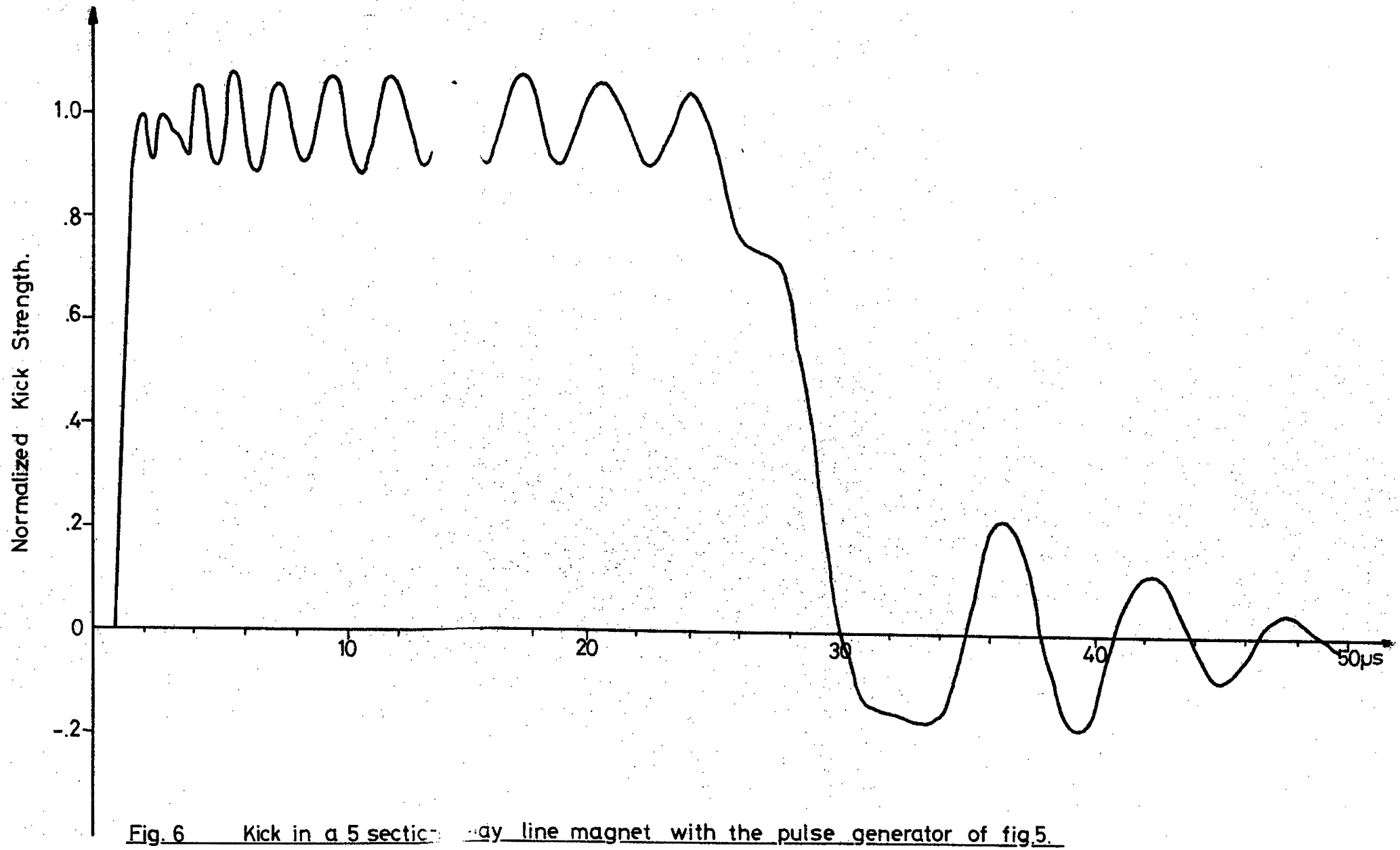

Fig. 6 Kick in a 5 sectic- -ay line magnet with the pulse generator of fig.5.

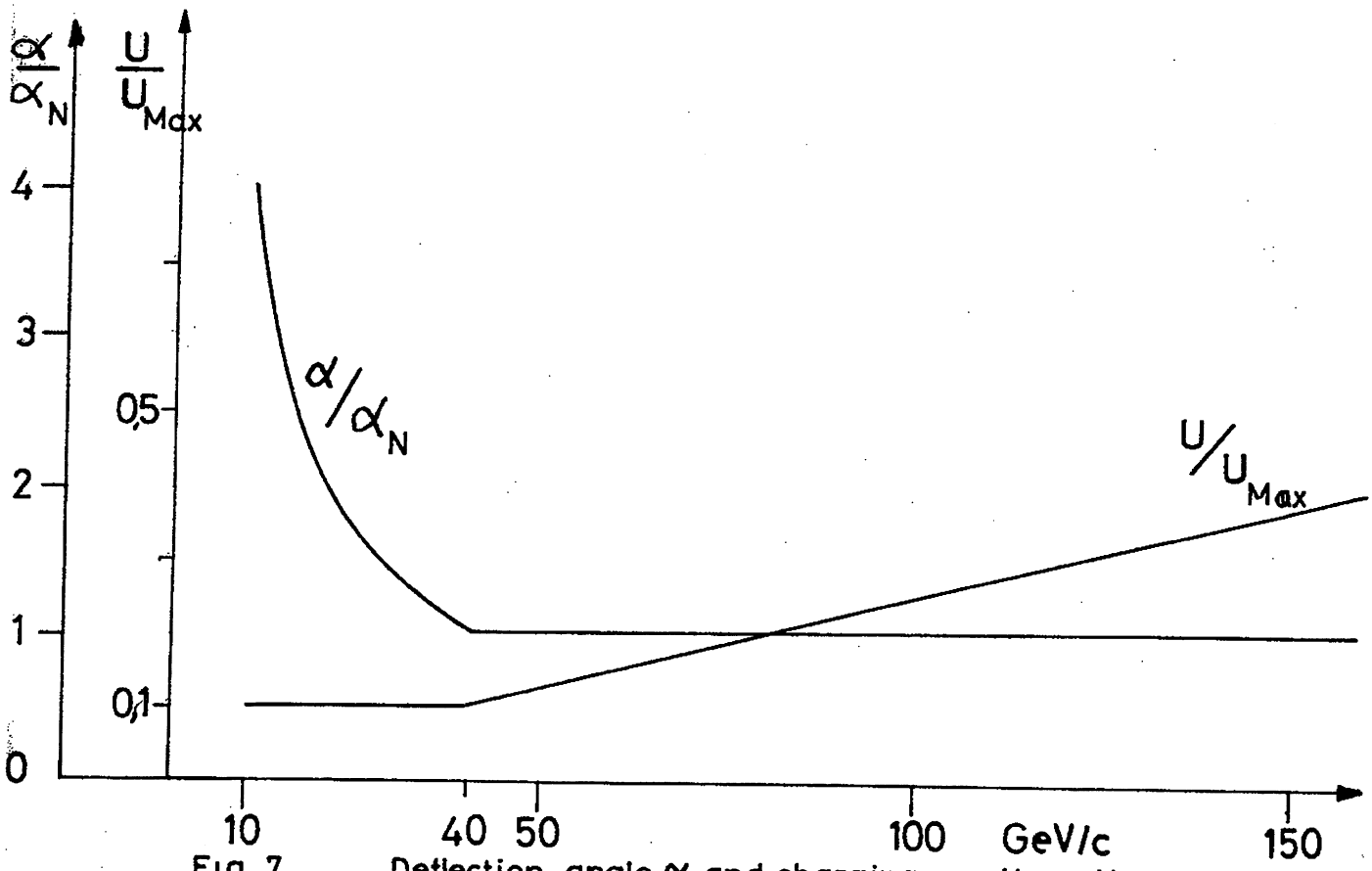

Fig 7 Deflection angle α and charging voltage U as function of momentum

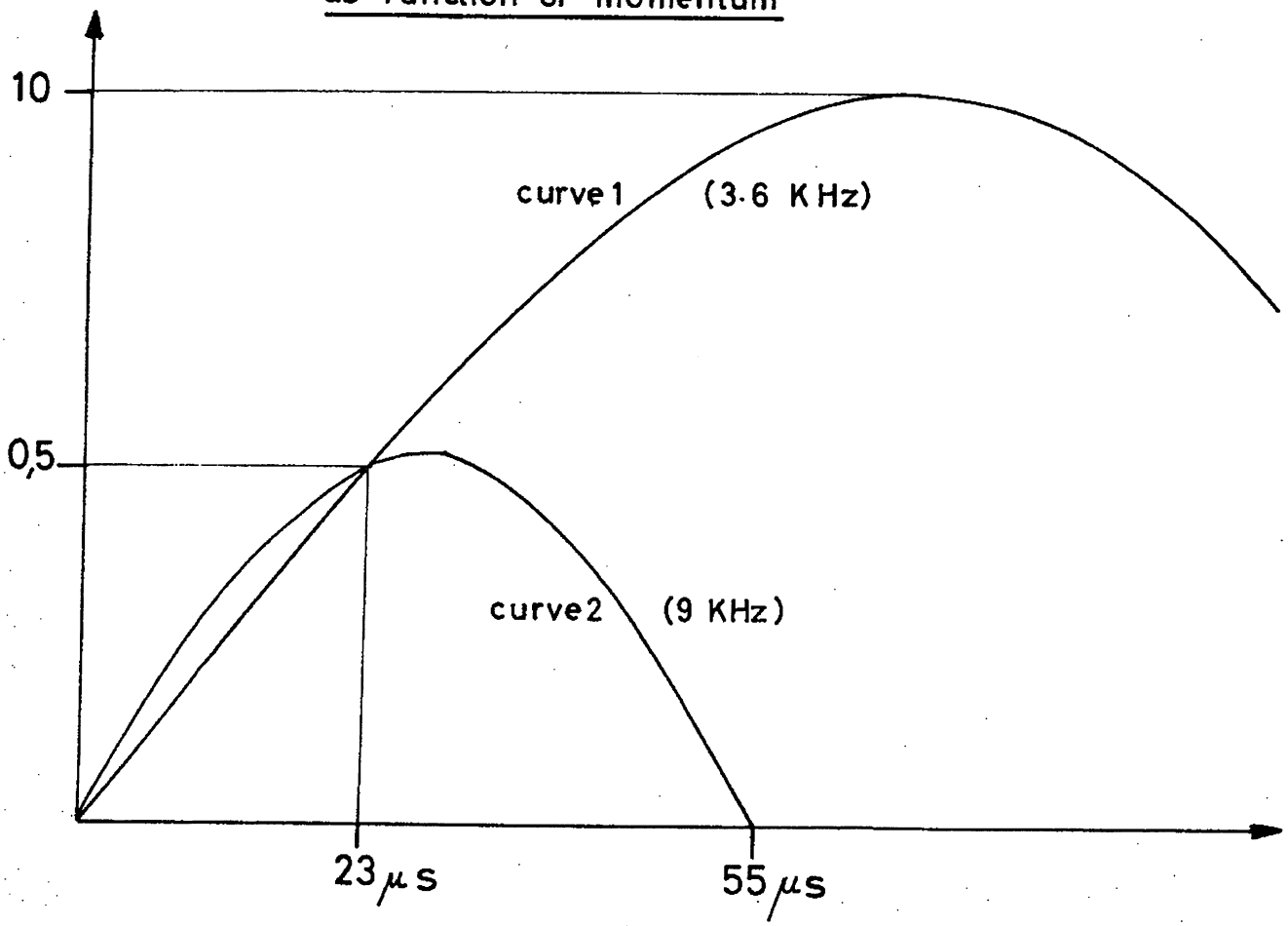

Fig 8 Rate of rise of excitation current

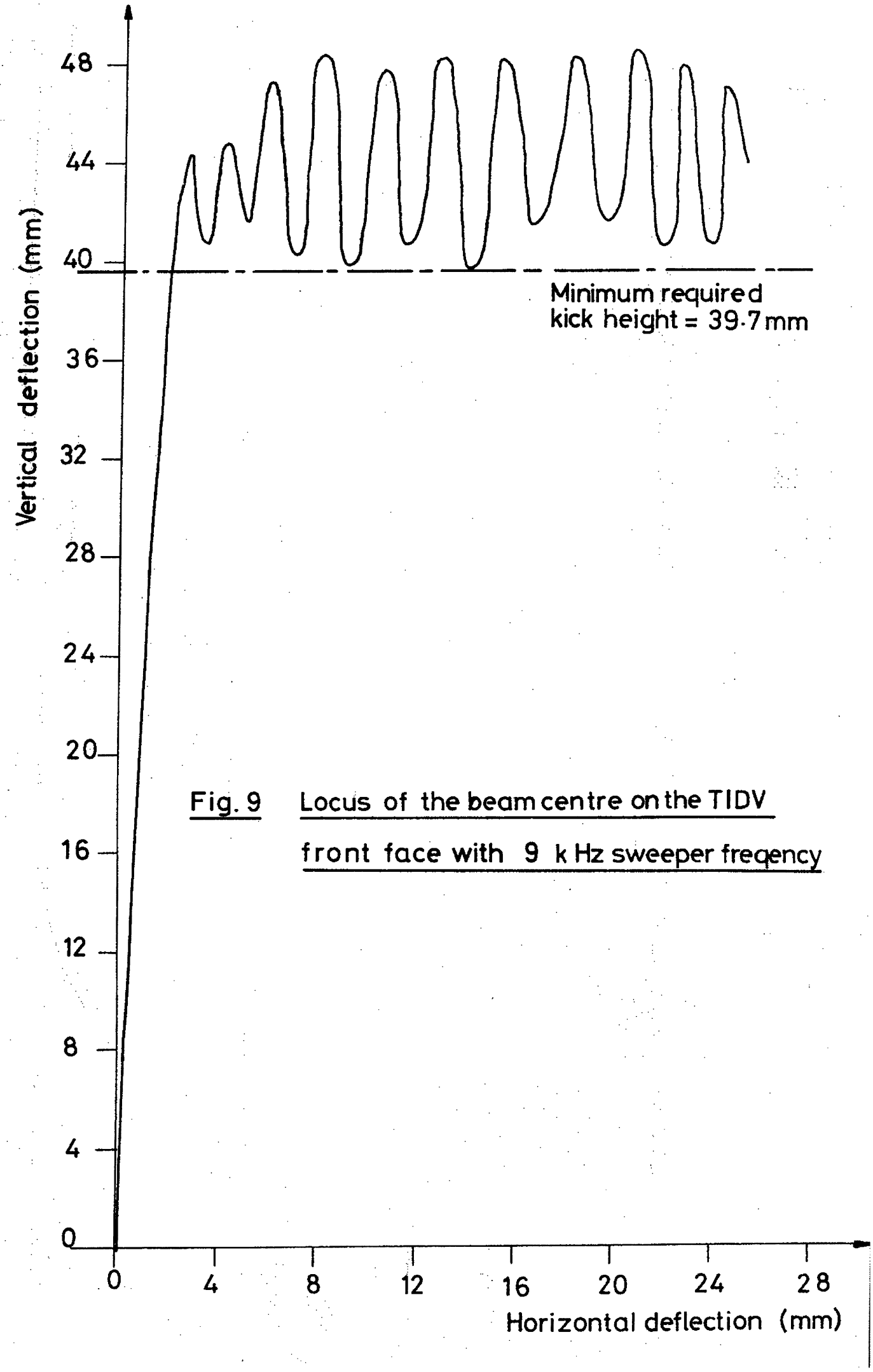

Fig. 9 Locus of the beam centre on the TIDV front face with 9 k Hz sweeper freqency

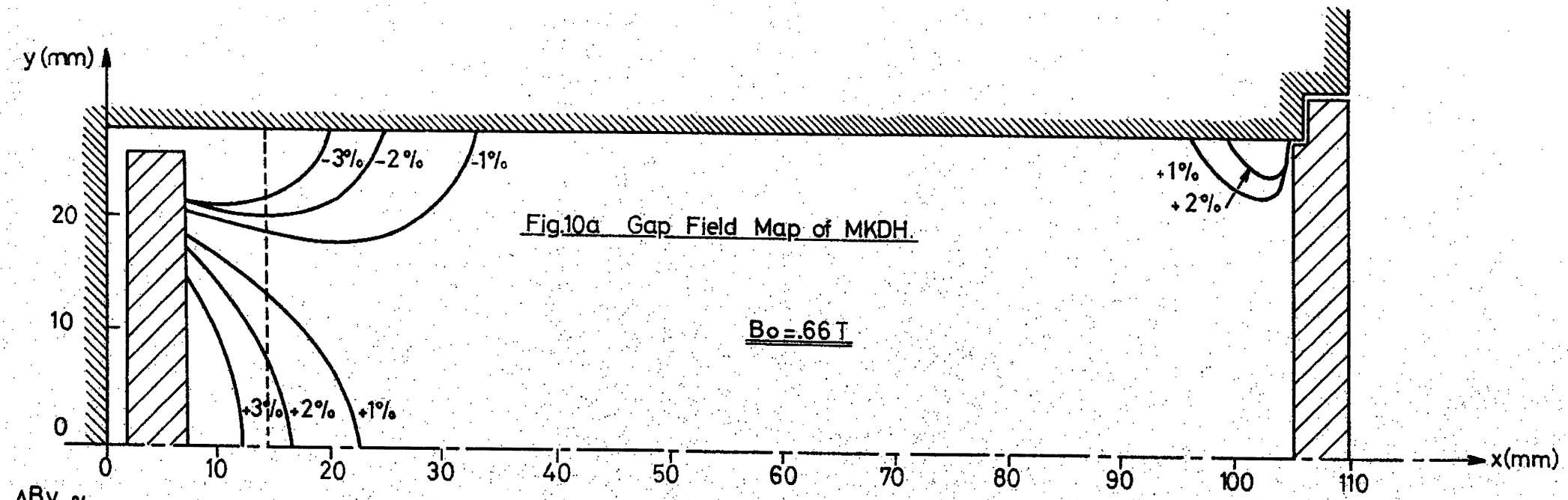

Fig.10a Gap Field Map of MKDH.

Bo=.66T

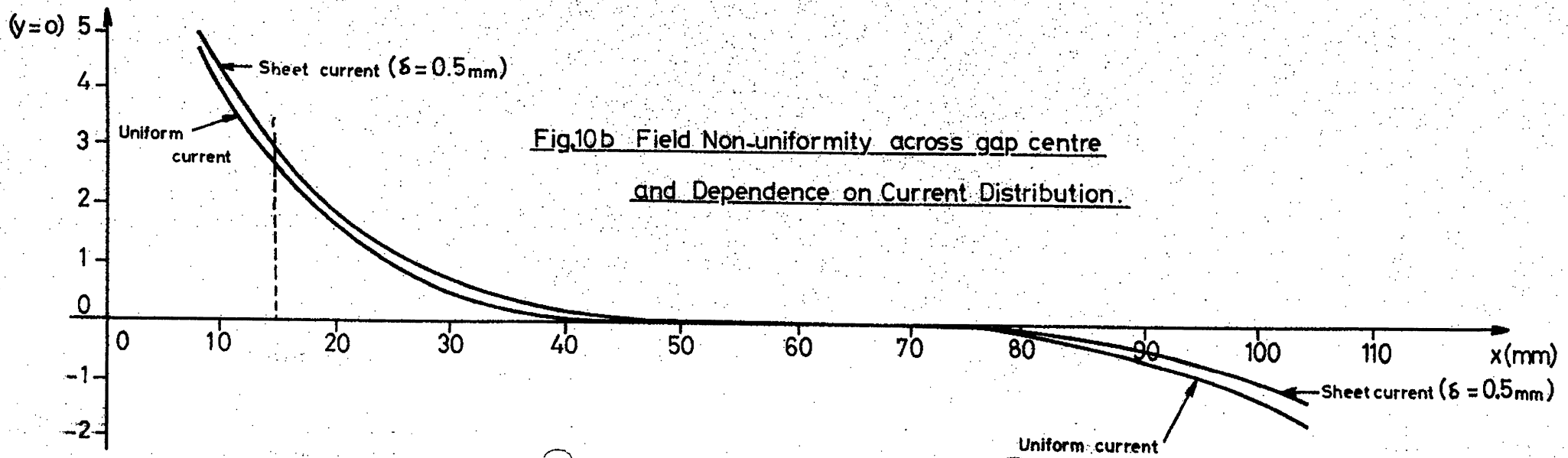

Fig.10b Field Non-uniformity across gap centre and Dependence on Current Distribution.

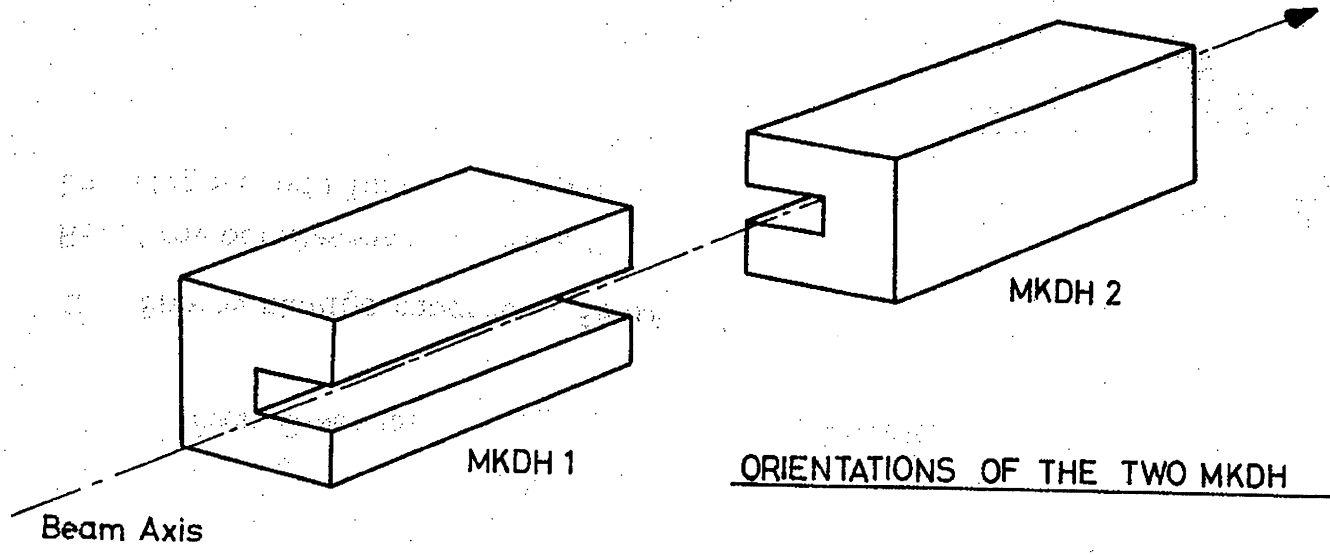

ORIENTATIONS OF THE TWO MKDH MAGNETS.

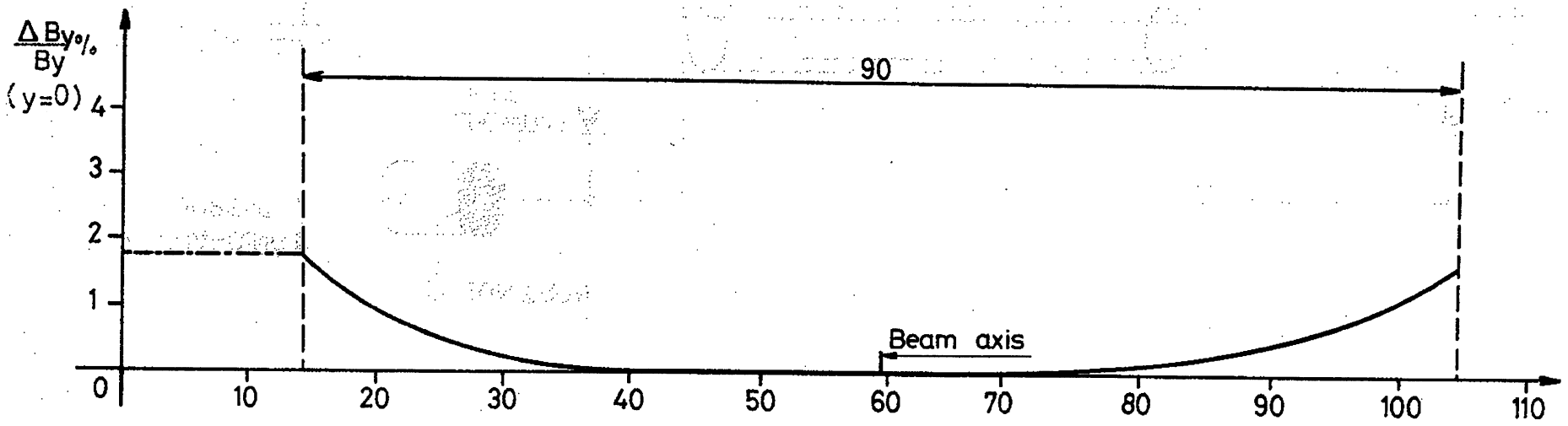

Fig.11 NET NON-UNIFORMITY OF THE FIELD DISTRIBUTIONS OF THE TWO MKDH MAGNETS. $\left(\frac{\Delta B}{B}\right)_{max} = +1.8\%$

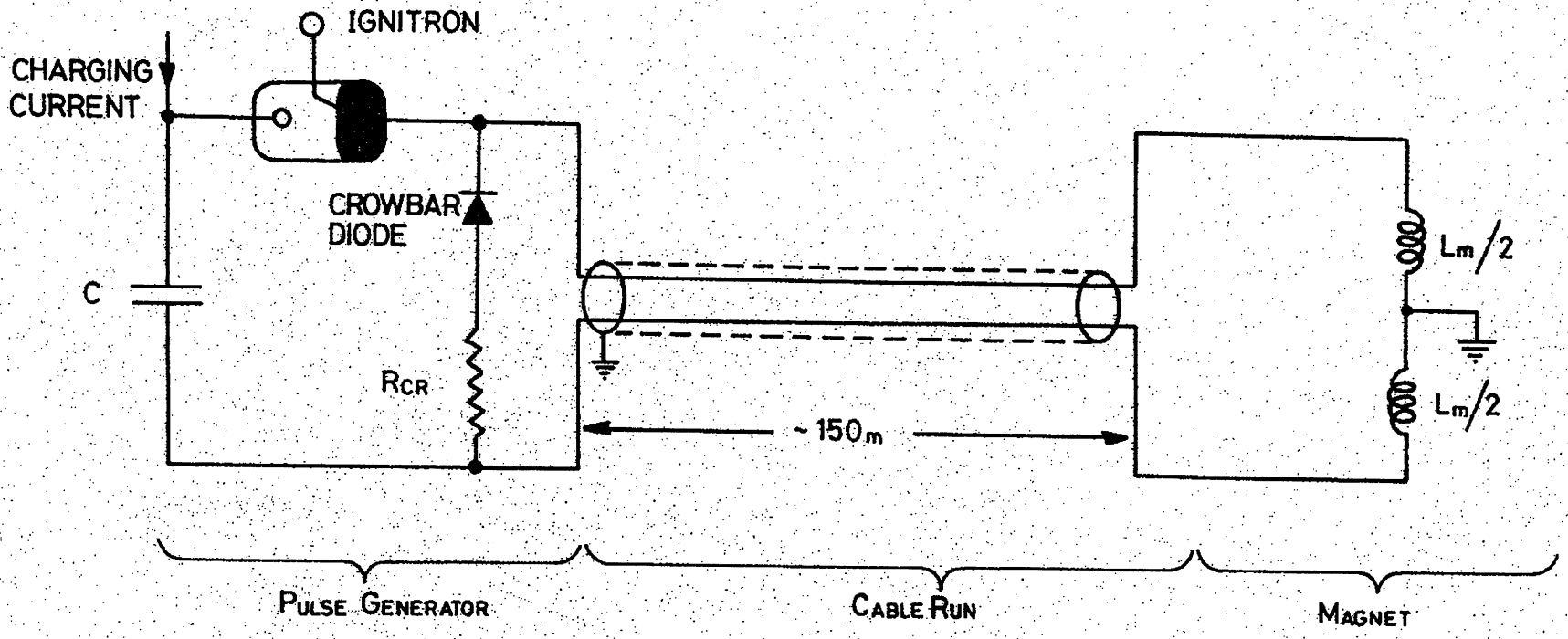

C : Energy storage capacitor ~66 μF

R_{CR} : Crowbar Resistor ~ 50 mΩ

Lm : Magnet inductance 2.4 μH

Fig.12 BASIC CIRCUIT DIAGRAM FOR THE SWEEPER MAGNET (MKDH).

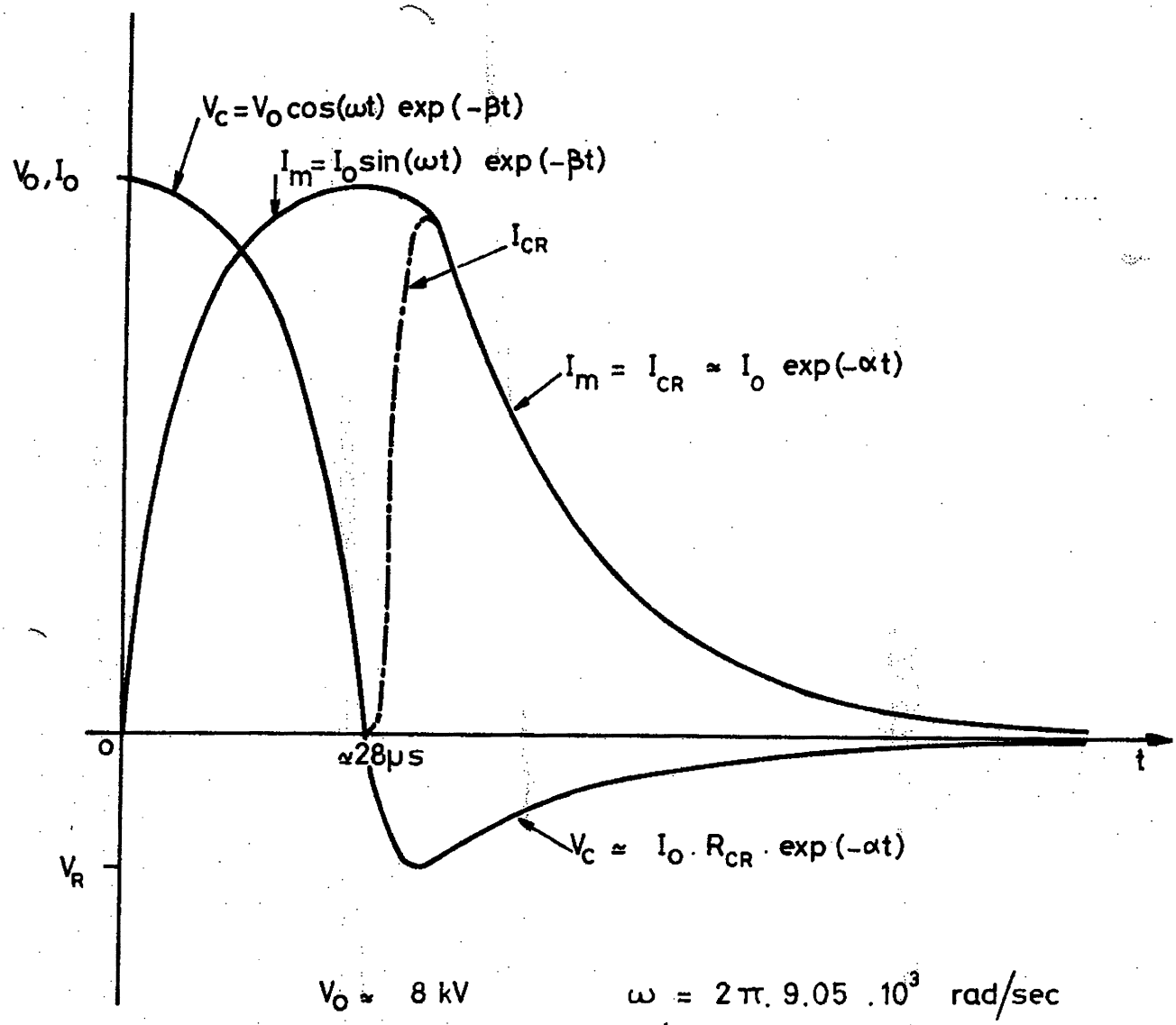

$V_O \simeq$ 8 kV

$I_O \simeq$ 30kA

Vc = capacitor voltage

Im = magnet current

I_{CR} = crowbar current

$\omega = 2\pi . 9.05 . 10^3$ rad/sec

$\alpha^{-1} = \frac{Lc + Lm}{R_{CR} + Rc} \simeq 50\ \mu s$

$\beta^{-1} = \frac{Lc + Lm}{Rc} \simeq 100\ \mu s$

Fig.13 BASIC WAVEFORMS IN THE CIRCUIT OF THE SWEEPER MAGNET (MKDH).